Numerical Simulation and Optimization of Methane Steam Reforming to Maximize H_2 Production: A Case Study

Estaner Claro Romao
Department of Basic and Environmental Sciences, Engineering College of Lorena, University of Sao Paulo, Brazil
estaner23@usp.br
(corresponding author)

Adriano Francisco Siqueira
Department of Basic and Environmental Sciences, Engineering College of Lorena, University of Sao Paulo, Brazil
adrianoeel@usp.br

Jairo Aparecido Martins
Department of Research & Development, DESCH North America, Canada
jairophd@gmail.com

Received: 29 December 2022 | Revised: 13 January 2023 and 16 January 2023 | Accepted: 20 January 2023

ABSTRACT

Research in renewable energy, the preservation of the environment, and the reduction of energy generation costs are themes that go hand in hand. In this work, a case study was carried out that aims to maximize the production of hydrogen through Methane Steam Reforming. For this, several numerical simulations, considering a laminar flow regime in a chemical reactor with a catalyst, were developed with COMSOL Multiphysics. After an exploratory study of the data, a systematic optimization was developed using multivariate regression models formed by combinations of input parameters in an idealized reactor. The results showed that the proposed approach is capable of satisfactory optimization.

Keywords-numerical simulation; hydrogen production; optimization; heat transfer

I. INTRODUCTION

Although modeling solute transport in porous media is not a new research branch since there are important records of models dated in 1952 and 1953 [1, 2], research of porous media has been thriving lately, mainly because it widened to solve inherent latent problems in the environmental, industrial, and biological sectors. Contamination of groundwater, diffusion of tracer particles in cellular bodies, underground oil flow in the petroleum industry, and even blow flow through capillaries are only a few relevant studies that have been bringing real and tangible contributions to the society [3, 4]. While the basic laws that govern the flow of fluids are accessible and usually make use of Navier-Stokes' equations, their application is not feasible for multiple complex geometries that are present in a detailed description of the pore structure of a realistic porous medium. This level of detail is not of practical use either, and ends up desiring a description at a level of detail somewhere intermediate between Darcy's law and the pore-level flow [3].

The numerical simulation is very important for solution several engineering problems [5-8], for example, authors in [9] presented numerical models for the resolution of density-coupled flow and transport in porous media based on mixed hybrid finite element and discontinuous finite element methods. The authors stated that the simulation presented a good agreement when tested against the standard benchmarks Henry and Elder test cases. Authors in [10] described heat and solute transport in porous media using partial differential equations of similar form, and the study happened to interpret two push-pull tests of different durations. The authors concluded that longitudinal solute dispersivity is scale-dependent while diffusivity seems not to be. Furthermore, the conductive transport of heat is much more important than the effects of velocity variations through the pore space. The contribution of the temperature in the process was studied in [11-12]. Authors in [13] stated that solutes having a limited mobilization in heterogeneous porous media may end up with subsurface salinization and clear contamination in various environmental

settings. Recent studies brought up that flow and transport driven by pressure waves in porous media under saturated conditions intensively enlarge solute displacement compared to drag-dominant (Darcy) flow and transport, resulting in more thorough remediation. However, the experimental results miss the demonstration of such transport under unsaturated conditions. The authors investigated solute leaching in a flow cell, experimentally modeling solute displacement from an unsaturated, saline, fine-textured soil region to the surrounding coarse-textured soil. They concluded stating that the Pressure-wave Pulse Flux (PPF) treatment led to higher water content at and behind the front, which increased the continuity of the water phase across the fine-textured and coarse-textured soils and enhanced transport. The study is a proof of concept for pressure-wave driven flow to enhance local wetting and solute transport in unsaturated soil.

When it comes to reactors, authors in [14] presented the thermochemical analysis of a packed-bed reactor via multi-dimensional CFD modeling using FlexPDE and COMSOL Multiphysics. The temperature, concentration, and reaction rate profiles for methane production following the Fischer–Tropsch (F-T) synthesis were studied. To this end, stationary and dynamic differential equations for mass and heat transfer were solved via the finite element technique. As a result, all models were in good agreement with the experimental data found in the literature, especially for the 2-D and 3-D dynamic models. In terms of kinetics, the predicted reaction rate profiles from the COMSOL model and the 2-D dynamic model followed the temperature trend, thus reflecting the temperature dependence of the reaction. Based on these findings, it was demonstrated that applying different approaches for the CFD modeling of F-T processes conducts reliable results.

Hydrogen production was studied in [15], since mechanically and chemically stable membranes with high perm-selectivity towards hydrogen are available and are continuously further improving in terms of stability and hydrogen flux. The authors highlight recent advances in hydrogen-selective membranes (from palladium-based to silica and proton conductors) along with the advances in the different types of membrane reactors available (from packed bed to fluidized bed and from micro-reactors to bio-membrane reactors). Meanwhile, the authors in [16] presented the catalytic reforming technology, which is regarded as one of the most popular hydrogen production methods. The introduction of a fluidized bed reactor provides a promising opportunity for the enhancement of catalytic reforming technology due to its good gas-solid contact and heat and mass transfer characteristics. The authors describe how, in order to improve hydrogen production, the strengthening method of reforming technology via hydrogen membrane separation has been developed in the last few years. The development and challenges of catalytic reforming technology using a membrane-assisted fluidized bed for hydrogen production are reviewed.

In the current work, we present a case study to present an alternative for optimizing an idealized chemical reactor. For this, we will use numerical simulations via COMSOL Multiphysics to solve the methane steam reforming chemical reaction given by:

$$CH_4 + H_2O \rightarrow CO + 2H_2 \quad (1)$$

which here will be considered irreversible since the main focus is the optimization of the idealized reactor.

II. METHODOLOGY

A. Parameters

Initially, we present the geometry of the case study. This is an idealized reactor with an inlet and an outlet, a region of porous medium (catalyst), and in its center there is a pipe through which a hot fluid passes, as can be seen in Figure 1.

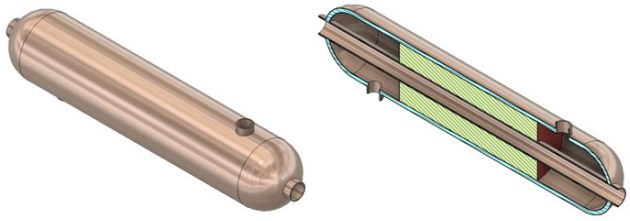

Fig. 1. Idealized reactor (left) and inside view of the reactor (right).

For the study presented here, the following characteristics will be considered:

- A two-dimensional study will be carried out and symmetry will be considered in the centerline of the idealized reactor (Figure 2), where L_1 is the length before the catalyst and the measurement between the hot fluid pipe and the reactor shell [m], L_R is the length of the catalyst region [m], L_2 is the length after the catalyst [m], U_0 is the inlet velocity [m/s], and T_{hot} is the temperature of the hot fluid [K].

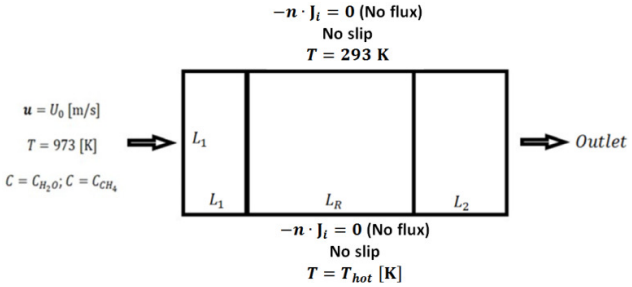

Fig. 2. Two-dimensional domain with boundary conditions.

- Porosity is considered equal to 0.5 and permeability to 10^{-9}m^2.
- The formula used to calculate the diffusivity between gases (D_{AB}) is [17]:

$$D_{AB} = 1{,}053 \times 10^{-3} \frac{T^{3/2}}{Pd^2{}_{AB}} \left[\frac{1}{M_A} + \frac{1}{M_B}\right]^{1/2} \quad (2)$$

where T is the temperature [K], P is the pressure [atm], M_A is the molar mass of element A (CH_4, H_2O, CO or H_2), M_B is the molar mass of element B (air) and d_{AB}, is defined by:

$$d_{AB} = (\sum \mathrm{v})_A^{1/3} + (\sum \mathrm{v})_B^{1/3} \quad (3)$$

In this work the values presented in Table I will be considered.

TABLE I. DIFFUSION MOLECULAR VOLUMES [13]

Molecule	Σv	Molar mass
Air	16.2	28.96
CO	18.0	28.01
H_2O	13.1	18.01
CH_4	25.14	16.033
H_2	6.12	2.016

- Due to the high activation energy required for the reaction proposed in (1) to occur, we will consider the inverse reaction to being negligible, and thus:

$$[H_2] = k[CH_4][H_2O] \quad (4)$$

$$[CO] = k[CH_4][H_2O] \quad (5)$$

where k is defined by (5) and using as reference [14], yields that:

$$k = 7.301 \times 10^{-2} e^{-\left(\frac{36150}{8,31 \times T}\right)} \quad (6)$$

B. Governing Equations

For the study of the conservation of motion, Brinkman's equations (laminar flow) will be used:

$$\nabla \cdot [-p\boldsymbol{I} + \boldsymbol{K}] - \left(\mu\kappa^{-1} + \beta\epsilon_p|\boldsymbol{u}| + \frac{Q_m}{\epsilon_p^2}\right)\boldsymbol{u} + \boldsymbol{F} \quad (7)$$

$$\rho\nabla \cdot \boldsymbol{u} = Q_m \quad (8)$$

More details about the terms of (9) and (10) can be found in [15]. Then, to carry out the study of mass transport in porous media, the following equations will be used:

$$\nabla \cdot \mathbf{J}_i + \boldsymbol{u} \cdot \nabla c_i = R_i + S_i \quad (9)$$

$$\mathbf{J}_i = -D_{e,j}\nabla c_i \quad (10)$$

$$\theta = \epsilon_p \quad (11)$$

More details about the terms of (9)-(11) can be found in [20]. Finally, for the treatment of the temperature field, the energy conservation equation will be used as follows:

$$d_z\rho C_p\boldsymbol{u} \cdot \nabla T + \nabla \cdot \mathbf{q} = d_z Q + q_0 + d_z Q_p + d_z Q_{vd} \quad (12)$$

$$\mathbf{q} = -d_z k\nabla T \quad (13)$$

More details about the terms of (12) and (13) can be found in [21].

III. RESULTS AND DISCUSSION

For the study that will be presented here, three parameters were chosen to be analyzed: the inlet concentration of H_2O [mol/m^3] (Case 1), the inlet velocity U_0 [m/s] (Case 2); and finally, the reactor length L_R [m] (Case 3). In all cases, the following parameters will be used as fixed: inlet concentration of CH_4 =1mol/m^3, L_1= 0.05m and L_2 =0.01m.

It is important to highlight that will be used the medium values of H_2 in the outlet of the idealized reactor in the results presented for the three cases.

A. Case 1: Varying H_2O

In the first case, we were varying the inlet concentration of H_2O in values between 1 and 1000mol/m^3. Besides, L_R = 0.1m and U_0 = 0.1m/s were fixed and 5 different values for T_{hot} were adopted: 973, 1023, 1073, 1123, and 1173K to verify the influence of hot fluid in the H_2 production.

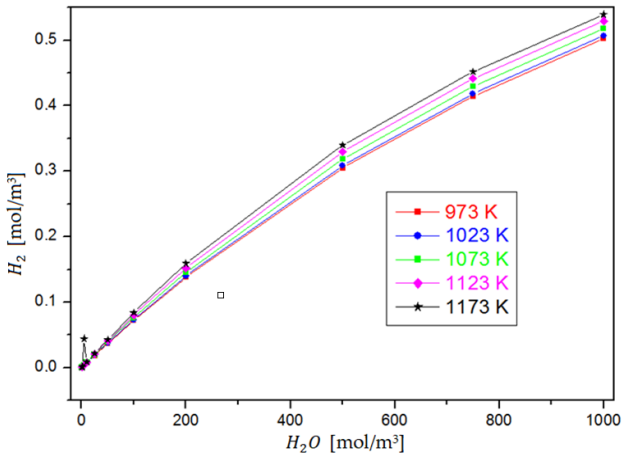

Fig. 3. H_2 production with H_2O (inlet) variation.

In Figure 3, it is possible to note that with the increasing inlet concentration of H_2O, increasing of the H_2 production occurs, however, it is clear that the results of the 5 different values of T_{hot} little differ. In Figure 4, it is clear that near in the region of heating the major concentration of H_2 production occurs.

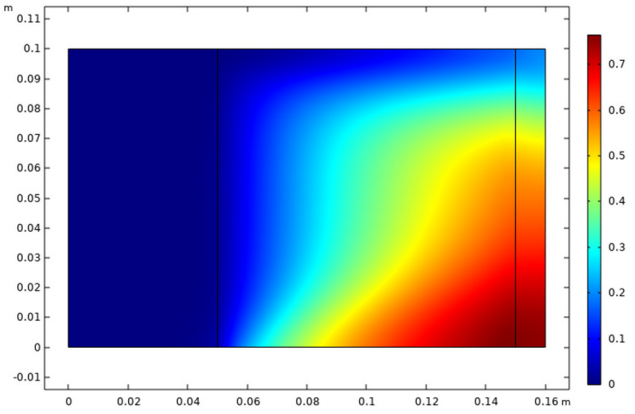

Fig. 4. H_2 concentration with H_2O = 1000mol/m^3 (inlet) and T_{hot} = 1173K.

B. Case 2: Varying U_0

In Case 1, it was clear that the major values adopted for H_2O and T_{hot} presented better results for H_2 production, thus, in Case 2 fixed values of H_2O = 1000mol/m^3 and T_{hot} = 1173K were adopted. From that, 11 different values of U_0 were be analyzed (of 0.005 to 0.1m/s). As in Case 1, L_R = 0.1m was considered. In Case 1 (Figure 3), within the values of H_2O inlet, the curves show crescent. The opposite occurs in Case 2 (Figure 5), since for the values adopted the curve shows a maximum point in the region of U_0 = 0.02m/s and then the curve becomes decreasing. In other words, the graph in Figure 5 suggests that the region near the U_0 = 0.02 is the possible optimum point.

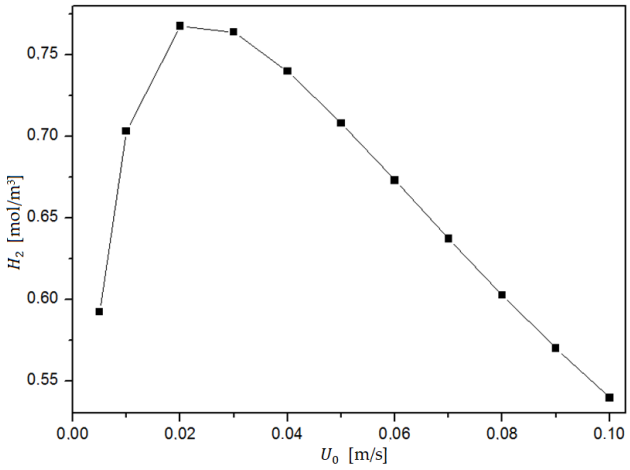

Fig. 5. H_2 production with U_0 variation.

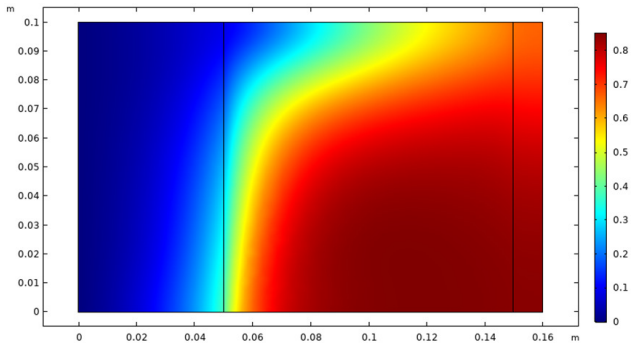

Fig. 6. H_2 concentration (Case 2) with $U_0 = 0.02$m/s.

Figure 6 shows that the H_2 production into the idealized reactor and is more expressive than that presented in Figure 4.

C. Case 3: Varying L_R

In this last case, L_R varied between 0.01 and 0.1m (10 points). Again, some values will be fixed: $T_{hot} = 1173$K and $H_2O = 1000$mol/m^3 (inlet). Besides, 3 values will be considered for U_0 (0.005, 0.01, and 0.02m/s).

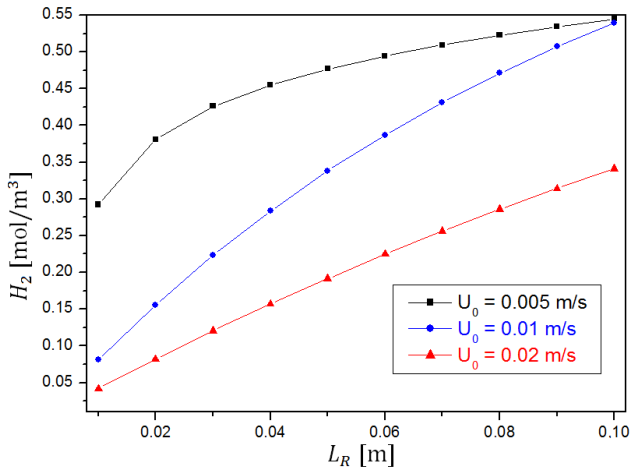

Fig. 7. H_2 production with L_R variation.

Although the three variations of U_0 were considered to present results expressibly different, the behavior is similar, that is, a behavior of the crescent curve, with a positive derivative and thus proving that the increase in L_R can still cause an increase in H_2 production.

D. Optimization

In order to understand the way the control parameters influence the generation of hydrogen through the chemical reaction proposed in this work (1), from the highest production, $H_2 = 0.767$mol/m^3 (found in the condition $L_R = 0.10$m, $U_0 = 0.02$m/s, $H_2O = 1000$mol/m^3, and $T_{hot} = 173$K among the data set analyzed in the 3 previously described cases), a new set of data was generated in the simulations, varying up and down by $p\%$ in the values of the input variables. The process was repeated, from the highest value found, generating a new data set with a sufficient number of points to test regression models with 3 independent variables and their 2 by 2 combinations, which, in this case, were 2 iterations using: $p = 0.1$ and (again) $p = 0.1$, thus forming a data set with 16 points. For this new data set, the best fit was obtained using the K-fold cross-validation with 10 folds. The model is expressed by (14):

$$H_2 = 0.5517 + 0.809L_R + 1.715U_0 + 0.000098H_2O \quad (14)$$

The statistics about the quality of fit of the model proposed by (14) are presented in Table II. We observe that the model fits very well to the simulated data, presenting high values of adjusted R2 and cross-validation, indicating that the model presents good capacity of generalization, with Anderson Darling test for normal residuals P-Value equal to 0.0864.

TABLE II. SUMMARY OF THE QUALITY MODEL FIT (14)

S	R2	R2(aj)	R2(pred)	10-fold S	10-fold R2
0.0045874	94.72%	93.50%	91.84%	0.0050580	91.61%

It is evident from the analysis of the P-value and the F-distribution (Table III) that the variable that most influences the generation of H_2 is the H_2O inlet concentration while the L_R length is the second more important.

TABLE III. ANALYSIS OF VARIANCE FOR THE PROPOSED MODEL OF (15)

	GL	SQ (Aj.)	QM (Aj.)	F-Value	P-Value
Regression	3	0.004910	0.001637	77.78	0.000
L_R	1	0.001337	0.001337	63.52	0.000
U_0	1	0.000269	0.000269	12.79	0.003
H_2O	1	0.002087	0.002087	99.16	0.000
Error	13	0.000274	0.000021		
Total	16	0.005184			

The quality of the fit can be seen in Figure 8. It is interesting to observe that the strategy of prospecting for new data in order to obtain a greater production of H_2 appears to be successful because it presents various combinations of L_R, U_0, and H_2O with H_2 greater than 0.767mol/m^3 from the initial dataset. Finally, using Minitab's optimizer, it is possible to envision a direction toward greater H_2 production. In Figure 9, it is evident that a greater production of H_2 can be obtained by increasing L_R, U_0, and H_2O. To assess whether these indications are correct, another simulation was performed in

that direction with $L_R = 0.125$m, $U_0 = 0.025$m/s, and $H_2O = 1250$mol/m^3 The simulation result was 0.823 and the prediction of the proposed model for these conditions was 0.818 with a prediction interval (95%) of [0.806, 0.830] showing the ability of the model to reproduce simulation data in laminar flow.

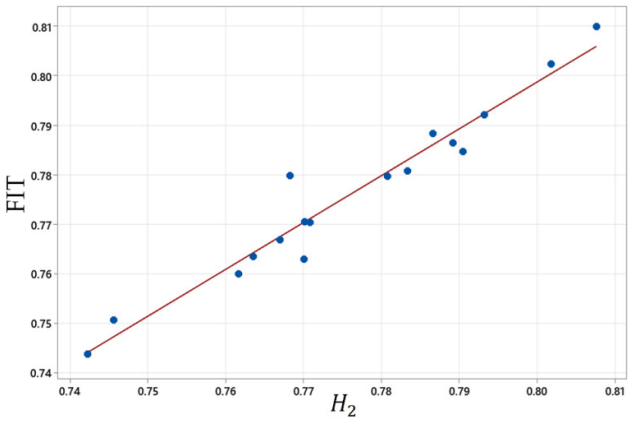

Fig. 8. Quality of model fit to simulated H_2 production data.

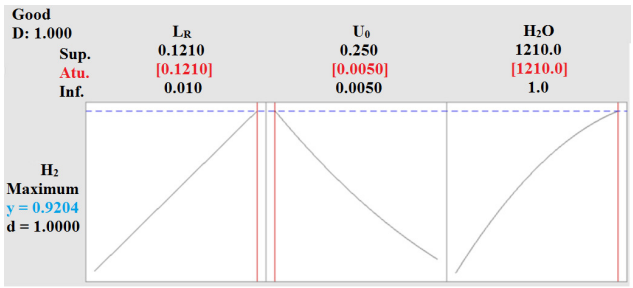

Fig. 9. Optimization of the proposed model to maximize H_2 production.

IV. CONCLUSIONS

The production of clean energy is one of the main themes nowadays and one of the available alternatives is the production of hydrogen. Although there are a considerable number of techniques and methods developed to design more efficient processes to produce hydrogen - many of them using only the Finite Element Method (FEM), others checking the results of FEM on experiments, the combination of numerical simulations with statistics is not observed in the literature. With that being said, the contribution of this paper is on demonstrating how this powerful combination can enhance the production of hydrogen since it allowed us to figure out precisely the significance of each variable in the system as well as the interaction among them.

In this work, we present an idealized reactor with a heating pipe that would carry out the chemical reaction known as methane steam reforming and generate hydrogen gas with the greatest efficiency. Through the variation of some physical and geometric parameters in the numerical simulation, we were able to present an optimization with high precision and high efficiency in the production of hydrogen by using statistics analysis. Besides, the statistical approach used in this work allowed finding a better optimal point than the one obtained in the initial exploratory numerical simulation analysis. It is important to point out that the use of statistics aimed at optimizing hydrogen production for the work proposed here is considered somewhat unprecedented since we did not find any work that used this approach.

In future work, an additional analysis could be carried out in maximizing the production of hydrogen with a possible reduction of CO (carbon monoxide) pollutant.

ACKNOWLEDGMENT

This research was funded by CAPES (Procs. 23038.000263/2022-19).

REFERENCES

[1] P. Daniel, "The measurement of groundwater flow," in *Proceedings of the Ankara Symposium on Arid Zone Hydrology*, 1952.

[2] G. I. Taylor, "Dispersion of soluble matter in solvent flowing slowly through a tube," *Proceedings of the Royal Society of London. Series A. Mathematical and Physical Sciences*, vol. 219, no. 1137, pp. 186–203, Jan. 1997, https://doi.org/10.1098/rspa.1953.0139.

[3] D. Kulasiri and W. Verwoerd, *Stochastic Dynamics. Modeling Solute Transport in Porous Media*, 1st ed. Amsterdam , Netherlands: Elsevier, 2002.

[4] Z. Shen, "Compactness and large-scale regularity for Darcy's law," *Journal de Mathématiques Pures et Appliquées*, vol. 163, pp. 673–701, Jul. 2022, https://doi.org/10.1016/j.matpur.2022.05.019.

[5] E. C. Romao and L. H. P. de Assis, "Numerical Simulation of 1D Unsteady Heat Conduction-Convection in Spherical and Cylindrical Coordinates by Fourth-Order FDM," *Engineering, Technology & Applied Science Research*, vol. 8, no. 1, pp. 2389–2392, Feb. 2018, https://doi.org/10.48084/etasr.1724.

[6] W. R. do P. Junior, J. A. Martins, and E. C. Romao, "Utilizing Numerical Simulations to Analyze the Efficiency of a Porous Reactor," *Engineering, Technology & Applied Science Research*, vol. 12, no. 3, pp. 8755–8759, Jun. 2022, https://doi.org/10.48084/etasr.4957.

[7] J. A. Martins and E. C. Romao, "The Importance of Accurate Boundary Condition in Obtaining Reliable Shearing Stresses on a Torsional Finite Element Simulation," *Engineering, Technology & Applied Science Research*, vol. 12, no. 3, pp. 8482–8487, Jun. 2022, https://doi.org/10.48084/etasr.4708.

[8] A. G. da Silva Jr, J. A. Martins, and E. C. Romao, "Numerical Simulation of a One-Dimentional Non-Linear Wave Equation," *Engineering, Technology & Applied Science Research*, vol. 12, no. 3, pp. 8574–8577, Jun. 2022, https://doi.org/10.48084/etasr.4920.

[9] Ph. Ackerer, A. Younes, and R. Mose, "Modeling Variable Density Flow and Solute Transport in Porous Medium: 1. Numerical Model and Verification," *Transport in Porous Media*, vol. 35, no. 3, pp. 345–373, Jun. 1999, https://doi.org/10.1023/A:1006564309167.

[10] A. Vandenbohede, A. Louwyck, and L. Lebbe, "Conservative Solute Versus Heat Transport in Porous Media During Push-pull Tests," *Transport in Porous Media*, vol. 76, no. 2, pp. 265–287, Jan. 2009, https://doi.org/10.1007/s11242-008-9246-4.

[11] H. R. Bravo, F. Jiang, and R. J. Hunt, "Using groundwater temperature data to constrain parameter estimation in a groundwater flow model of a wetland system," *Water Resources Research*, vol. 38, no. 8, pp. 28-1-28–14, 2002, https://doi.org/10.1029/2000WR000172.

[12] T. Keesari *et al.*, "Tracing thermal and non-thermal water circulations in shear zones of Eastern Ghats Mobile Belt zone, Eastern India- inferences on sustainability of geothermal resources," *Journal of Hydrology*, vol. 612, Sep. 2022, Art. no. 128172, https://doi.org/10.1016/j.jhydrol.2022.128172.

[13] D. Kalisman, A. Yakirevich, S. Sorek, and T. Kamai, "Enhancing solute transport by pressure-wave driven flow in unsaturated porous media," *Journal of Hydrology*, vol. 612, Sep. 2022, Art. no. 128196, https://doi.org/10.1016/j.jhydrol.2022.128196.

[14] S. Taco-Vasquez, C. A. Ron, H. A. Murillo, A. Chico, and P. G. Arauz, "Thermochemical Analysis of a Packed-Bed Reactor Using Finite Elements with FlexPDE and COMSOL Multiphysics," *Processes*, vol. 10, no. 6, Jun. 2022, Art. no. 1144, https://doi.org/10.3390/pr10061144.

[15] F. Gallucci, E. Fernandez, P. Corengia, and M. van Sint Annaland, "Recent advances on membranes and membrane reactors for hydrogen production," *Chemical Engineering Science*, vol. 92, pp. 40–66, Apr. 2013, https://doi.org/10.1016/j.ces.2013.01.008.

[16] X. Yang, S. Wang, and Y. He, "Review of catalytic reforming for hydrogen production in a membrane-assisted fluidized bed reactor," *Renewable and Sustainable Energy Reviews*, vol. 154, Feb. 2022, Art. no. 111832, https://doi.org/10.1016/j.rser.2021.111832.

[17] M. A. Cremasco, *Difusão Mássica - Cremasco*. Blucher, 2019.

[18] Y. Wang and C. M. Kinoshita, "Kinetic model of biomass gasification," *Solar Energy*, vol. 51, no. 1, pp. 19–25, Jul. 1993, https://doi.org/10.1016/0038-092X(93)90037-O.

[19] "The Brinkman Equations Interface," *COMSOL*. https://doc.comsol.com/5.6/doc/com.comsol.help.cfd/cfd_ug_fluidflow_porous.10.37.html.

[20] "The Chemistry Interface." https://doc.comsol.com/5.6/doc/com.comsol.help.chem/chem_ug_chemsptrans_re.07.31.html.

[21] "The Heat Transfer in Fluids Interface," *COMSOL*. https://doc.comsol.com/6.0/doc/com.comsol.help.heat/heat_ug_interfaces.08.20.html.